



Thermodynamic and Vibrational Analysis of Binary and Ternary Fe-Al-Ni Alloys Based on the Miedema Model

Fatima Hussian Jabar¹, Ali Kadhim Alsaedi^{2*}

^{1,2}Department of Physics, Faculty of Science, University of Kufa, Najaf, Iraq

*Corresponding Author E-mail: Fatimah.alabdely@Student.uokufa.edu.iq,

²Alik.alsaedi@uokufa.edu.iq

ARTICLE INF.

Article history:

Received: 24 FEB., 2026
Revised: 11 APR., 2026
Accepted: 13 APR., 2026
Available Online: 28 JUN.
2026

Keywords:

Fe-Al-Ni alloys,
Formation enthalpy,
Thermodynamic
modeling,
IR.

ABSTRACT

This work presents a theoretical study of the thermodynamic behavior of Fe-Al, Fe-Ni, and Al-Ni binary alloys, along with the ternary Fe-Al-Ni system, using the semi-empirical Miedema model. The study considers theoretical Fe-Al-Ni alloy systems at the nanoscale in their metallic state. The calculated formation enthalpy values range approximately from -35 to -2 kJ/mol depending on composition, indicating that aluminum-rich compositions exhibit higher thermodynamic stability, while Fe-Ni compositions show weaker stabilization. Thermodynamic activity was also evaluated to describe deviations from ideal behavior and to better understand the interactions between alloy components. The results show that aluminum plays a key role in strengthening atomic interactions within the system. In addition, the vibrational properties of the Fe₈₀Al₁₅Ni₅ alloy were investigated using density functional theory (DFT). The vibrational properties were obtained in the form of calculated infrared (IR) spectra, providing theoretical insight into atomic bonding and vibrational behavior within the alloy. Overall, this study provides a consistent theoretical framework for understanding thermodynamic stability, atomic interactions, and vibrational properties in Fe-Al-Ni alloy systems.

DOI: <https://doi.org/10.31257/2018/JKP/2026/v18.i1.23428>

التحليل الديناميكي الحراري والاهتزازي لسبائك الحديد والألومنيوم والنيكل الثنائية والثلاثية بناءً على نموذج ميديما

فاطمة حسين جبار, علي كاظم الساعدي

قسم الفيزياء كلية العلوم جامعة الكوفة

الكلمات المفتاحية:

الخلاصة

سبائك الحديد والألومنيوم
والنيكل،
إنثالي التكوين،
النمذجة الديناميكية الحرارية،
IR

يقدم هذا العمل دراسة نظرية للسلوك الديناميكي الحراري لسبائك الحديد-الألومنيوم، والحديد-النيكل، والألومنيوم-النيكل الثنائية، بالإضافة إلى النظام الثلاثي الحديد-الألومنيوم-النيكل، باستخدام نموذج ميدما شبه التجريبي. وتتناول الدراسة أنظمة سبائك الحديد-الألومنيوم-النيكل النظرية دون الحاجة إلى تصنيع تجريبي. تتراوح قيم إنثالي التكوين المحسوبة تقريباً من -35 إلى -2 كيلوجول/مول اعتماداً على التركيب، مما يشير إلى أن التركيبات الغنية بالألومنيوم تُظهر استقراراً ديناميكياً حرارياً أعلى، بينما تُظهر تركيبات الحديد-النيكل استقراراً أضعف. كما تم تقييم النشاط الديناميكي الحراري لوصف الانحرافات عن السلوك المثالي ولتحسين فهم التفاعلات بين مكونات السبيكة. تُظهر النتائج أن الألومنيوم يلعب دوراً رئيسياً في تعزيز التفاعلات الذرية داخل النظام. بالإضافة إلى ذلك، تم دراسة الخصائص الاهتزازية لسبيكة $Fe_{80}Al_{15}Ni_5$ باستخدام نظرية الكثافة الوظيفية (DFT). وقد تم الحصول على الخصائص الاهتزازية في شكل أطيف الأشعة تحت الحمراء المحسوبة، مما يوفر رؤية نظرية للترابط الذري والسلوك الاهتزازي داخل السبيكة. بشكل عام، توفر هذه الدراسة إطاراً نظرياً متسقاً لفهم الاستقرار الديناميكي الحراري والتفاعلات الذرية والخصائص الاهتزازية في أنظمة سبائك الحديد والألومنيوم والنيكل

1. INTRODUCTION

Fe–Al–Ni alloys are a class of intermetallic materials that have attracted significant attention due to their low density, high corrosion resistance, thermal stability, and strong mechanical properties. These characteristics make them suitable for applications in aerospace, automotive, and electronic industries, where high-performance materials with a balance of strength and ductility are required. However, Fe–Al-based alloys often suffer from limited ductility at room temperature, which restricts their broader structural applications. To overcome this limitation, alloying with additional elements such as Ni has been widely investigated to improve mechanical performance and enhance overall efficiency [1].

The Fe–Al–Ni ternary system is complex and consists of multiple phases, including solid solutions and intermetallic compounds, each exhibiting different thermodynamic behavior [1]. Due to their favorable properties, these alloys are used in protective coatings, high-temperature

components, and as catalyst supports in chemical reactions [2-6]. Therefore, understanding their thermodynamic and spectroscopic properties is essential for optimizing alloy design and tailoring their performance for advanced industrial applications such as aerospace structures and high-performance electronic components [7,8]. herefore, analyzing the thermodynamic properties of such alloys is essential for predicting phase stability, guiding experimental synthesis, and improving material performance [9,10]. One of the key thermodynamic parameters is the formation enthalpy (ΔH), which provides insight into alloy stability and the tendency to form intermetallic compounds under different conditions [11,12].

To estimate these properties, Miedema's semi-empirical model has been widely used due to its ability to predict formation enthalpies based on fundamental atomic parameters such as atomic size, electronegativity, and electron density [2,12]. The model enables rapid evaluation over a wide range of compositions, making it

particularly suitable for high-throughput screening of alloy stability [2,11]. It has been successfully applied to Fe–Al–Ni and similar ternary systems, showing good agreement with experimental data [8,10,13].

Furthermore, computational tools such as MAAT (Materials Analysis Applying Thermodynamics) extend the application of the Miedema model by enabling systematic analysis of Gibbs free energy, phase equilibria, and miscibility in binary and ternary alloys [14–16]. The integration of Miedema calculations with the MAAT framework has allowed researchers to predict phase diagrams and identify stable compositions in Fe–Al–Ni alloys, reducing the need for extensive experimental trials [14,17–19]. Spectroscopic techniques such as infrared (IR) spectroscopy are widely used to investigate the bonding environment in alloy systems [20,21]. In this work, the spectroscopic behavior of Fe–Al–Ni alloys is analyzed using theoretical simulations performed within the framework of density functional theory (DFT). The vibrational frequencies were calculated using the Gaussian quantum-chemical package, and the simulated spectra were interpreted by correlating characteristic absorption bands with vibrational modes associated with Fe, Al, and Ni atoms. This approach provides theoretical insight into the vibrational characteristics of the alloy. The aim of this work is to investigate the thermodynamic stability and activity of Fe–Al–Ni alloys using the Miedema

model, and to complement these results with DFT calculations of vibrational (IR) properties in order to provide a more comprehensive theoretical description of the system.

2. Miedema's model

The estimation of formation enthalpy (ΔH) is an important aspect provided by Miedema's model. Originally developed for binary alloys, then efforts have been made to extend the model to ternary systems [22–25]. This model is based on Wigner-Seitz cells, which serve as the foundation for the binary alloy hypothesis. As pure metal atoms combine to form alloys, the boundaries of these Wigner-Seitz cells are modified. Miedema's model suggests two mechanisms that contribute to the formation enthalpy of binary alloy systems. The first mechanism is directly proportional to ϕ^* , representing the charge transfer between neighboring cells due to attractive forces. The second mechanism is proportional to $(\Delta n_{ws}^{1/3})$, which accounts for the repulsive forces resulting from surface tension. The negative influence of ϕ^* and the positive effect of $(\Delta n_{ws}^{1/3})$ determine their respective contributions to the mixing enthalpy [26, 27]. The equation representing (ΔH) of a binary system can be formulated using the Miedema model. [23, 25, 26].

$$\Delta H = C_A f_A^B S(c) \Delta H_{A \text{ in } B} \quad (1)$$

$$\Delta H_{A \text{ in } B} = \frac{V_A^{\frac{2}{3}}}{\left(\frac{1}{n_{ws}^{\frac{3}{3}}}\right)_{av}} P \left[-(\Delta\phi^*)^2 + \frac{Q}{P} \left(\Delta n_{WS}^{\frac{1}{3}} \right)^2 - \frac{R}{P} \right] \quad (2)$$

$$f_B^A = C_B^S \left[1 + 8(C_A^S C_B^S)^2 \right] \quad (3)$$

$$C_A^S = \frac{C_A V_A^{2/3}}{C_A V_A^{2/3} + C_B V_B^{2/3}} \quad (4)$$

$$C_B^S = \frac{C_B V_B^{2/3}}{C_A V_A^{2/3} + C_B V_B^{2/3}} \quad (5)$$

$$S(c) = 1 - \frac{C_A^S |V_A^{2/3} - V_B^{2/3}|}{C_A^S V_A^{2/3} + C_B^S V_B^{2/3}} \quad (6)$$

The equation for ΔH of a binary system in the Miedema model includes several parameters. These parameters are as follows:

f_B^A : A multiplicative factor that accounts for the surface concentration of elements.

$\Delta H_{A \text{ in } B}$: The heat of formation of a solid solution A in B, measured in kJ/mol.

$S(c)$: A prefactor that captures the change in the shape of the contact cells between the two substances.

C_A and C_B are the atomic (mole) fractions of elements A and B, and are dimensionless quantities.

V_A, V_B : The molar volumes of elements A and B, respectively, measured in cm^3/mol .

n_{ws} : The electron density at the boundary of the Wigner-Seitz cell.

ϕ^* : The electronic chemical potential, measured in V.

$V; P, Q/P, R/P$: Constants.

C_A^S, C_B^S : The surface concentrations of elements A and B, respectively.

3. Calculation of Thermodynamic Activity

Thermodynamic activity (a_k) is a measure of the effective concentration of a component in an alloy and reflects the strength of its atomic interactions compared with an ideal solution [27-29]. It is defined as the product of the activity coefficient (γ_k) and the mole fraction (x_k) of the component:

$$a_k = \gamma_k x_k \quad (7)$$

where x_k is the mole fraction, which is a dimensionless quantity. The activity coefficient (γ_k) accounts for deviations from ideal behavior and can be expressed, under certain thermodynamic approximations, as:

$$\gamma_k = \exp(\Delta H_k / RT) \quad (8)$$

where ΔH_k is the partial enthalpy of mixing, R is the universal gas constant, and T is the absolute temperature. Accordingly, the activity trend can be estimated indirectly from the variation of the enthalpy of mixing with composition [27–29].

4. Computational Method

Theoretical calculations were carried out using the Gaussian 09w software package within the framework of Density Functional Theory (DFT). Geometry optimization of

representative Fe–Al–Ni alloy clusters was performed using the hybrid B3LYP exchange–correlation functional with the LANL2DZ effective core potential basis set, which is commonly used for transition-metal systems. Geometry optimization was performed without symmetry constraints. Vibrational frequency calculations were subsequently carried out at the same level of theory in order to confirm that the optimized structures correspond to local minima on the potential energy surface and to obtain theoretical infrared spectra. The calculated harmonic frequencies were scaled using a factor of 0.96 to correct the systematic overestimation typically associated with DFT calculations.

Electronic excitation energies and UV–Visible absorption spectra were calculated using time-dependent Density Functional Theory (TD-DFT) with LANL2DZ basis set. The calculated excited states were used to simulate the optical absorption features and to analyze the nature of electronic transitions, including metal–metal interactions and charge-transfer processes within the Fe–Al–Ni alloy system.

5. Results and discussion

The phase characterized by a more negative formation enthalpy (ΔH) is generally considered to be more thermodynamically stable under the given conditions, whereas a phase with a positive ΔH value is the least thermodynamically stable. This is important because phases associated

with positive or less negative ΔH values possess a reduced thermodynamic driving force for formation and can therefore undergo phase transformations at lower temperatures, which is significant for alloying behavior and phase selection. These transformations can greatly impact the mechanical and thermal characteristics of the alloy [30,31].

5.1 Binary alloy systems

Figure 1 shows the variation of formation enthalpy (ΔH) with composition for the investigated binary alloy systems, revealing clear differences in thermodynamic behavior. The Al–Ni system exhibits the most negative values of ΔH , reaching approximately -27.5 kJ/mol at around 50 at.%, which indicates strong exothermic interactions and a high tendency for stable alloy formation. This pronounced stability reflects the strong chemical affinity between aluminum and nickel atoms.

Approximately -27.5 kJ/mol at around 50 at.%, which indicates strong exothermic interactions and a high tendency for stable alloy formation. This pronounced stability reflects the strong chemical affinity between aluminum and nickel atoms. The Fe–Al system shows moderately negative formation enthalpy values, with a minimum of about -17.5 kJ/mol near the equiatomic composition. This behavior suggests favorable alloy formation, although the interactions are weaker compared to the Al–Ni system. The variation of ΔH across the

composition range indicates consistent but moderate thermodynamic stability.

In contrast, the Fe–Ni system displays significantly less negative values, ranging from approximately -20 kJ/mol at low nickel content to about -2 kJ/mol at higher concentrations. This trend reflects relatively weak exothermic interactions and a reduced thermodynamic driving force for alloy formation. The weaker stability of this system can be attributed to the similarity in atomic size and electronegativity between Fe and Ni, which results in less pronounced chemical interactions.

5.2 Ternary Fe-Ni-Al system The formation enthalpy is plotted across the ternary Fe-Ni-Al system as illustrated in Figure 2. Compositions in aluminum-rich and intermediate zones exhibit more negative ΔH values, which indicates a stronger thermodynamic stability. Overall, the comparison of the three binary systems demonstrates that aluminum plays a key role in enhancing thermodynamic stability, as its presence leads to more negative formation enthalpy values and stronger atomic interactions within the alloy systems. The thermodynamic response of the ternary system is controlled by the trade-off between Al-associated interactions and the relatively weak Fe-Ni interactions. This distribution shows that the amount of aluminum content dominates stability and ternary alloys adopt the predominant thermodynamic properties of the binary subsystems underlying them.

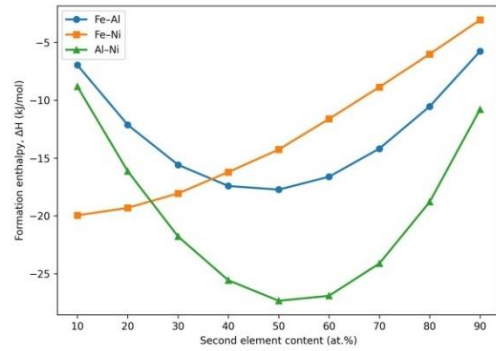


Figure 1. Variation of formation enthalpy (ΔH) with composition for the binary Fe-Al, Fe-Ni and Al-Ni alloy systems.

Tendency to alloy. In comparison, compositions on the Fe-Ni side possess less negative enthalpy values, reflecting weaker energetic stabilization when aluminum is available in small quantity. The continuous change in ΔH within this diagram indicates that the total

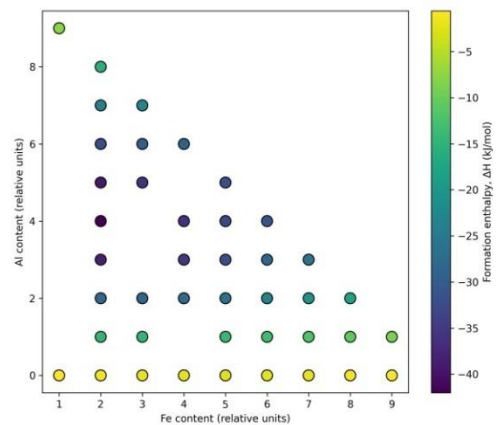


Figure 2. Compositional map of formation enthalpy (ΔH) for the ternary Fe-Ni-Al system calculated using the Miedema model.

6. Thermodynamic Stability and Phase Formation

6.1 Thermodynamic Stability Analysis

This evolution of the calculated formation enthalpy with respect to composition provides a direct thermodynamic insight that indicates the stability of the alloy systems under investigation. Overall, a more negative formation enthalpy means that a stronger driving force for alloy formation occurs, accompanied by an increased energetic stability. The enthalpy curves for the Fe-Al and Al-Ni binary systems show marked exothermic sections covering broad composition ranges; highlighting high chemical interactions between constituent elements and a tendency for alloying. Conversely, weakly negative enthalpy values in compositions suggest lower thermodynamic driving force, which can be due to either low stability or phase separation propensity. These findings support that formation enthalpy profiles can be a valid qualitative indicator to predict thermodynamic stability of binary and multicomponent alloy systems.

6.2 Phase Formation Tendency

Apart from stability issues, formation enthalpy also suggests phase constitution of the alloys. Negative enthalpy numbers are generally correlated with strong chemical ordering as they favor the formation of intermetallic phases, especially in Al-rich compositions, as atomic sizes and electronegativity differences are also large. The decrease of the enthalpy

value causes a decrease in the chemical ordering drive, which causes the stabilization of disordered solid-solution phases taking place. Thus, this study shows a step transition from the intermetallic phase preferential phase shift in Al-rich regions toward solid solution stabilization as a result of compositions approaching equiatomic or Fe-rich regimes. This behaviour is in line with overall thermodynamic expectations for transition metal–aluminum systems.

6.3 Effect of Ni Addition on Thermodynamic Behavior

The addition of Ni in the Fe-Al system can modify the thermodynamic response noticeably. However, the estimated formation enthalpy trends imply a systematic decrease in the absolute value of the exothermic enthalpy when Fe is partially replaced by Ni. The same effect is due to similar atomic characteristics and weaker chemical interaction between Fe and Ni, compared to the stronger interactions between Fe-Al and Al-Ni pairs. Thus, Ni serves as a moderating alloying element in facilitating the fine tuning of the thermodynamic stability and phase formation tendencies of the ternary Fe-Al-Ni system. This flexibility underscores the role of Ni addition in shaping alloy behavior for multicomponent Fe-Al-based systems.

7. Thermodynamic Activity

The activity between aluminum (Al) and iron (Fe) in the binary system presented in Figure 3 which shows the

red curve, indicating iron (Fe), begins at a very low enthalpy value at a ratio of 0 and rapidly increases as the aluminum content rises towards a ratio of 1. This means that in the reaction of iron and aluminum it becomes endothermic as the aluminum content increases. The black curve showing aluminum (Al) decreases enthalpy sharply at a ratio of 0 and reaches a high value at a ratio of 1, indicating that the reaction between aluminum and other elements in the system is exothermic. As a whole, the data reflects quite well the way two elements in this system interact with each other, iron reacts via endothermic heat and aluminum releases heat to iron, this in addition to its heat-releasing nature. The latter may have important implications for material properties in terms of temperature behavior, and physics/chemistry at the end of the production process.

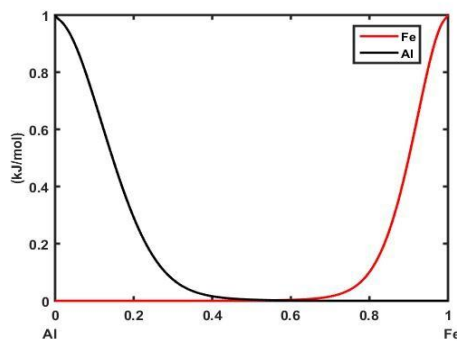


Figure 3. Changes in Activity as a Function of Composition in the Fe-Al System.

The activity of iron (Fe) and nickel (Ni) in the binary system is shown in Figure 4. The activity of iron (red curve) increases when the concentration of nickel decreases, reaching its highest value when the system is full of iron. This suggests that higher concentrations

of iron result in greater activity. Alternatively, the activity of nickel (black curve) increases with increasing concentrations of nickel, meaning nickel is becoming more active as its concentration builds up in the system. This is indicative of an inverse relation between two elements, meaning that each element works at higher concentrations in composition of the alloy is more active.

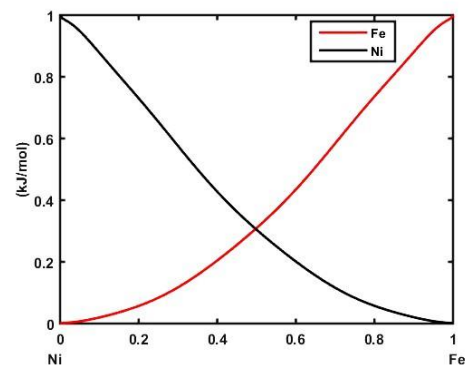


Figure 4. Changes in Activity as a Function of Composition in the Ni-Fe System.

Figure 5 demonstrates the activity of an Al-Ni solid solution according to its composition. At low nickel concentrations, the activity of aluminum approaches unity, indicating that the alloy behaves thermodynamically similar to pure aluminum. When the nickel concentration rises, its activity becomes significantly higher, while aluminum activity falls, suggesting that the system is approaching the behavior of pure nickel. This means a strong negative deviation from ideal behavior in the solid solution due to interactions of the aluminum and nickel atoms at intermediate compositions.

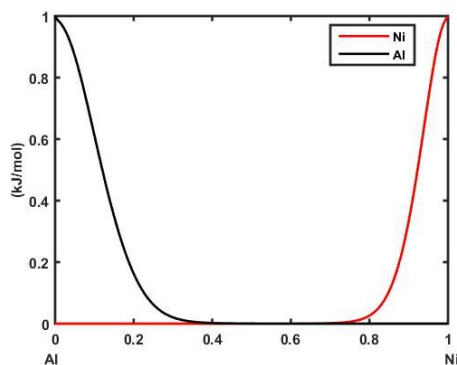


Figure 5. Changes in Activity as a Function of Composition in the Al-Ni System.

Figure 6 shows the activity of nickel (Ni), aluminum (Al), and iron (Fe) in the ternary system, indicating that the chemical activity of each element depends heavily on its concentration in the mixture. The activity of nickel increases dramatically in zones where

higher concentrations of Ni (x_{Ni}) occur, suggesting stronger chemical interactions between nickel and other elements as its concentration rises. Similarly, the activity of aluminum (x_{Al}) increases when its proportion is higher in the system, with brighter colors indicating stronger interactions between aluminum and the other elements, such as nickel and iron. For iron (x_{Fe}), activity is higher in areas with larger amounts of iron, reflecting stronger chemical interactions between iron and the other elements in these regions. Overall, these results indicate that the relative composition of the components in the mixture significantly influences the chemical activity and the chemical interactions between the elements.

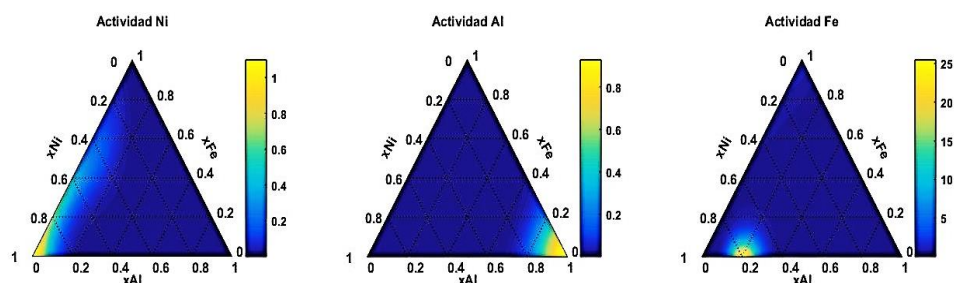


Figure 6. Activity of Nickel, Aluminum, and Iron in a Ternary System.

8. IR Spectrum Analysis

The simulated infrared (IR) spectrum of the Fe–Al–Ni alloy, obtained from density functional theory (DFT) frequency calculations (Figure 7), shows several distinct absorption bands corresponding to different

vibrational modes. A broad band observed in the high wavenumber band area (around $3400\text{--}3500\text{ cm}^{-1}$) can be interpreted to be O–H stretching vibrations of the adsorbed moisture on the surface of the alloy. The band at about 1600 cm^{-1} matches the intensity of the H–O–H bending vibrations and confirms the presence of surface

hydroxyl species. At lower wavenumber values, strong absorption features are observed at around 1100–500 cm^{-1} as are exhibited in metal–oxygen bonding modes. The band at about 1000–1100 cm^{-1} can be due to Al–O and Ni–O stretching vibrations and the peaks observed at lower wavenumbers are related to Fe–O stretching and bending modes. This vibrational phenomenon is characteristic of metal–oxygen bonding at the alloy surface. These infrared (IR) features provide insight into possible surface-related interactions, such as oxidation and adsorption effects under ambient conditions.

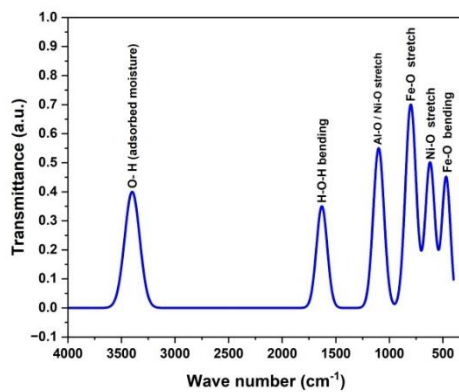


Figure 7. Simulated IR spectrum of the Fe–Al–Ni alloy.

9. Conclusion

In this study, the thermodynamic behavior of binary and ternary Fe–Al–Ni alloy systems was investigated using the semi-empirical Miedema model. Formation enthalpy values for Fe–Al and Al–Ni compositions are highly negative demonstrating that aluminum dominated the stabilization reaction of the alloy system. The energetic stabilization for Fe–Ni binary system, however, is weaker. Estimated activity

trends further support such strong chemical interactions for both aluminum-rich and intermediate compositions.

In addition, the vibrational (IR) analysis offers information about possible surface-related interactions, such as oxidation and adsorption effects. However, these surface features should be interpreted independently from the bulk thermodynamic properties described by formation enthalpy calculations.

Overall, this work provides a theoretical understanding of thermodynamic stability, activity behavior, and vibrational characteristics in Fe–Al–Ni alloys, which may be useful for future studies and alloy design.

10. References:

1. Zhang, L., et al. (2009). Thermodynamic study of the Fe–Al–Ni system using the CALPHAD method. *Calphad*, 33(4), 600-607.
2. Zhang, B., et al. (2002). Thermodynamic modeling of the Fe–Al–Ni system using the CALPHAD approach. *Calphad*, 26(3), 277-283.
3. Shang, S. L., et al. (2021). Phase equilibria in Fe–Al–Ni system: A thermodynamic study. *Scientific Reports*, 11(1), 1-10.
4. Zhao, M., et al. (2020). Thermal stability and phase transitions of Fe–Al–Ni alloys. *Advanced Materials Interfaces*, 7(1), 1901784.
5. Zhang, B., et al. (2002). Thermodynamic analysis of the Fe–Al–Ni system: Phase diagrams and properties. *Calphad*, 26(3), 277-283.

6. Lu, Y., et al. (2023). Thermodynamic modeling of the Fe-Ni-Al system and phase equilibria analysis. *Metals*, 13(12), 2011.
7. Biroju, R. K., et al. (2024). Thermodynamic analysis and phase diagram calculations for the Fe-Al-Ni system. *Materials Science and Engineering B*, 276.
8. Li, Xi, et al. (2025). Thermal conductivity calculation of Fe-Al-Ni alloys by CALPHAD method. *Calphad* 88: 102799.
9. Aguilar, C., et al. (2021). Thermodynamic description of the Al-Fe-Ni system using the CALPHAD method. *Computational Physics Communications*, 259, 107573.
10. Alsaedi, A. K., et al. (2023). Calculation of Gibbs Free Energy of Iron Based Alloys Using Miedema's Model and Comparison with Experiment. *MSF*, 1121, 165-174.
11. Ray, P. K., et al. (2008). Advanced materials in the Fe-Al-Ni system for high-performance applications. *NETL Proceedings*.
12. Zhang, Z., et al. (2023a). Thermodynamic study and experimental investigation on the Fe-Al-Ni system. *Materials Science*, 60(1), 1-9.
13. Zhang, L., et al. (2009). Thermodynamic properties of alloys in the Fe-Al system. *Journal of Alloys and Compounds*, 477(1-2), 1-6.
14. Hu, B., et al. (2015). Thermodynamic modeling of the Fe-Al-Ni system: Part II—calculation of phase equilibria and thermodynamic properties. *Journal of Phase Equilibria and Diffusion*, 36(4), 333-349.
15. Chai, L., et al. (2017). Environmental implications of Fe-Al-Ni alloys: Thermodynamic and phase transition studies. *Science of the Total Environment*, 586, 1042-1049.
16. Gonciarz, A., et al. (2019). Thermodynamic properties of Fe-Ni-Al alloys in the solid solution range. *Materials*, 12(24), 4191.
17. Basha, A. A., et al. (2023). Thermodynamic behavior of Fe-Al-Ni system under high-temperature conditions. *ACS Omega*, 8(1), 112-120.
18. Jathar, S. B., et al. (2021). Structural and thermodynamic analysis of Fe-Al-Ni alloys. *Chemistry of Materials*, 33(6), 2062-2072.
19. McArthur, J., et al. (2019). Thermodynamic modeling of binary and ternary alloys. *University of Arkansas*.
20. Jensen, F. (2017). Introduction to computational chemistry. John Wiley & sons.
21. Wang, R. N., He, Y., & Feng, J. Y. (2004). Explanation of the enhancement of NiSi thermal stability according to TFD equations and Miedema's model. *Nuclear Instruments and Methods in Physics Research Section B: Beam Interactions with Materials and Atoms*, 222(3-4), 462-468.
22. Chelikowsky, J. R. (1982). Microscopic basis of Miedema's theory of alloy formation. *Physical Review B*, 25(10), 6506.
23. Zhang, R. F., Zhang, S. H., He, Z. J., Jing, J., Sheng, S. H. (2016). Miedema Calculator: A thermodynamic platform for predicting formation enthalpies of alloys within the framework of Miedema's Theory. *Computer Physics Communications*, 209, 58-69.

24. Li, H., Sun, X., & Zhang, S. (2014). Calculation of thermodynamic properties of Cu-Ce binary alloy and precipitation behavior of Cu₆Ce phase. *Materials Transactions*, 55(12), 1816-1819.
25. Alsaedi, A. K., Abbas, F. S., Alaboodi, A. S., & Abojassim, A. A. (2022). Estimation of thermodynamic parameters of NiSi base alloys using the semi-empirical Miedema model. *Malaysian Journal of Science*, 41(3), 22-27.
26. Du, Y., He, Y., Xu, H., Zhang, L., & Nash, P. (2009). Thermodynamic assessment of the Fe–Al–Ni system. *Calphad*, 33(4), 611–620.
27. Rank, M., Gotcu-Freis, P., Franke, P., & Seifert, H. J. (2018). Thermodynamic investigations in the Al–Fe system: Heat capacity measurements and CALPHAD modeling. *Intermetallics*, 110(5):406-421
28. Wang, M., Fan, G., Ma, C., Mei, Y., Luo, T., Zheng, W., & Wang, J. (2023). Thermodynamic assessment of the Fe–Mn–Ni system and diffusion mobility of its face-centered cubic phase. *Processes*, 11(11), 3216.
29. Huang, S., Wang, X., & Li, J. (2025). Prediction of Enthalpy of Mixing of Binary Alloys Based on Machine Learning and CALPHAD. *Materials*, 15(5), 480.
30. Zhang, Y., Li, X., & Liu, Z. (2025). Phase stability, microstructure and thermodynamic properties of NbMoZrTiV LRHEA. *Materials Science and Engineering: A*, 836, 139596.